

Full-polaron master equation approach to dynamical steady states of a driven two-level system beyond the weak system-environment coupling

Chien-Chang Chen,¹ Thomas M. Stace,² and Hsi-Sheng Goan^{1,3,*}

¹*Department of Physics and Center for Theoretical Physics,
National Taiwan University, Taipei 10617, Taiwan*

²*ARC Centre for Engineered Quantum Systems, School of Mathematics and Physics,
The University of Queensland, Brisbane, Queensland 4072, Australia*

³*Center for Quantum Science and Engineering, National Taiwan University, Taipei 10617, Taiwan*
(Dated: July 20, 2020)

We apply a full-polaron master equation and a weak-coupling non-Markovian master equation to describe the steady-state time-averaged properties of a driven two-level system, an electron coherently tunneling between double quantum dots (DQDs), interacting with a bosonic phonon bath. Comparing the results obtained using these two master equations with those from a recent DQD experiment and its corresponding weak-coupling theoretical method, we find that the original parameter set used in the experiment and theoretical method is not in the weak-coupling parameter regime. By using the full-polaron master equation with a slight adjustment on only the value of the interdot separation in the original experimental parameter set, we find that a reasonable fit to the experimentally measured time-averaged steady-state population data can be achieved. The adjusted interdot separation is within the possible values allowed by the geometry of the surface gates that define the DQD in the experiment. Our full-polaron equation approach does not require the special renormalization scheme employed in their weak-coupling theoretical method, and can still describe the experimental results of driving-induced phonon-enhanced steplike shoulder behaviors in the experiment. This demonstrates that the full-polaron master equation approach is a correct and efficient tool to describe the steady-state properties of a driven spin-boson model in the case of strong system-environment coupling.

I. INTRODUCTION

Dynamics of driven open quantum systems is of broad interest and great importance for many different fields and disciplines ranging from quantum information processing to biological physics. For a standard spin-boson model with a two-level energy splitting $\hbar W$ and an environment-induced decay rate Γ proportional to the system-bath coupling strength P , the master equation approach [1] via weak-coupling perturbation with respect to P is one of the most often adopted approaches to treat open quantum systems. This approach is valid in the weak coupling regime, i.e., small P such that $W \gg \Gamma$. While for a spin-boson model sinusoidally driven at frequency ω_0 , even though $W \gg \Gamma$, this perturbation process may fail under the weak driving and near or on resonance conditions [2] where $\max(\Omega_0, |\delta|) \ll \Gamma$, step-like with Ω_0 being the driving amplitude and $|\delta| = |W - \omega_0|$ being the detuning.

Quantum dots are promising physical systems for coherence control experiments due to their great controllability and tunability [3, 4]. In this paper, we investigate a driven double quantum-dot (DQD) system in a recent experiment [5]. When the DQD is driven such that the driving amplitude Ω_0 is comparable to the energy scale of system-environmental coupling, a steplike shoulder may appear on the blue-detuned off-resonant side ($W < \omega_0$) of the resonance peak. The asymmetry of

the line shape of the sidebands indicates the interaction with the environment as excitation channels are opened when $\omega_0 > W$ [5–7]. The experiment in Ref. [5] showed this clear asymmetry and steplike shoulder feature on the blue side of the sideband and theoretical work based on a weak system-environment coupling theory [7] was put forward to explain the observed feature in Ref. [5].

In this paper, we use both a weak system-environment coupling treatment and a full-polaron transformation approach serving as a strong system-environment coupling treatment to study the driven DQD system interacting with a phonon bath described in Ref. [5]. We find that the parameters of the driven DQD system used in Ref. [5] are beyond the weak system-environment coupling regime. However, the theoretical method [7] employed in Ref. [5] to explain the experiment involves only second-order perturbation theory in the system-bath interaction. Therefore, using the full-polaron method valid for strong system-environment coupling, we find that to fit the experimental data, only one critical parameter, the interdot separation, adopted in Ref. [5] for their theory, is required to be adjusted by a small magnitude. The adjusted interdot separation is still consistent with the distance and geometry of the surface gates that confine and define the DQD system as shown in Ref. [5].

The paper is organized as follows. We describe in Sec. II the model Hamiltonian for the driven DQD system, and then present the derivations of our weak-coupling and full-polaron master equations. Numerical results are presented in Sec. III, in which we compare our two master-equation approaches with the ex-

* Email: goan@phys.ntu.edu.tw

periment data [5]. A comparison between the approach in Refs. [5, 7] and our weak-coupling and full-polaron master-equation approaches is presented in Sec. IV. Then a short conclusion is given in Sec. V. Finally, we discuss the validity of the parameter set of the driven DQD system used in Ref. [5] in Appendix A and the problem of positivity violations in second-order master equations in Appendix B.

II. MODEL HAMILTONIAN AND NON-MARKOVIAN MASTER EQUATION

The system considered in the experiment [5] is an electron in a DQD system driven by a microwave at frequency ω_0 and amplitude Ω_0 . There is an energy bias ϵ between localized left $|l\rangle$ and localized right $|r\rangle$ states of the DQD, and the electron tunnels coherently between the DQD with interdot tunneling rate Δ . Furthermore, the DQD system is coupled to its surrounding bosonic bath and the total Hamiltonian describing the whole system [7] is ($\hbar = 1$):

$$H_T(t) = H_s(t) + H_b + H_{sb}, \quad (1)$$

$$H_s(t) = -\frac{\epsilon}{2}\sigma_z - \frac{\Delta(t)}{2}\sigma_x, \quad (2)$$

$$H_b = \sum_k \omega_k b_k^\dagger b_k, \quad (3)$$

$$H_{sb} = \sigma_z \sum_k g_k (b_k^\dagger + b_k), \quad (4)$$

where $\sigma_z \equiv |l\rangle\langle l| - |r\rangle\langle r|$, $\sigma_x \equiv |l\rangle\langle r| + |r\rangle\langle l|$, and

$$\Delta(t) = \Delta - 2\Omega_0 \cos(\omega_0 t). \quad (5)$$

Here, the DQD is treated as a two-level system (qubit) with Hamiltonian H_s , the Hamiltonian for the bosonic bath is H_b with frequency ω_k and creation (annihilation) operator b_k^\dagger (b_k) of the bath modes, and H_{sb} is the system-bath interaction Hamiltonian with strength g_k coupling to the respective bath mode k . Next, we will describe how our weak-coupling and the polaron master equations are obtained and then use them to compare with the experimental data.

A. Weak-coupling non-Markovian master equation

First, we introduce a master equation valid to second order in system-bath coupling strength and at the same time valid for a strong driving field. We will adopt the weak-coupling time-nonlocal (time-convolution) non-Markovian master equation [8, 9] to describe the time evolution of the reduced density matrix of the system

$$\dot{\rho}_s(t) = \text{tr}_b[\rho_T(t)] \quad (6)$$

to compare directly with that in Ref. [7] as a time-nonlocal non-Markovian master equation was used there.

Because we focus on the comparison of the steady-state population with the experiment [5], and in our case the dynamical steady-state result is independent of any reasonable choices of initial states, the initial total density operator is, for simplicity, taken to be $\rho_T(0) = |l\rangle\langle l| \otimes \rho_b$, i.e., the electron in the DQD localized in the left state $|l\rangle\langle l|$ and the bath in the thermal equilibrium state $\rho_b = e^{-\beta H_b} / \text{tr}_b e^{-\beta H_b}$. The time-nonlocal master equation to second order in system-bath interaction strength in the interaction picture reads [8]

$$\frac{d}{dt}\tilde{\rho}_s(t) = -\int_0^t \text{tr}_b \left[\tilde{H}_{sb}(t), \left[\tilde{H}_{sb}(t'), \tilde{\rho}_s(t') \otimes \rho_b \right] \right] dt', \quad (7)$$

where $\tilde{H}_{sb}(t) = \mathcal{G}_s(0, t) \sigma_z B(t)$, $B(t) = \sum_k g_k (b_k^\dagger e^{i\omega_k t} + b_k e^{-i\omega_k t})$. The propagator superoperator $\mathcal{G}_s(t, t')$ has a general form of

$$\mathcal{G}_s(t, t') \equiv T_+ \exp \left[\int_{t'}^t \mathcal{L}_s(t'') dt'' \right], \quad (8)$$

with T_+ denoting the time-ordering operator necessary to allow an explicit time-dependent Hamiltonian [8], and the Liouville superoperator

$$\mathcal{L}_s(t) A \equiv -i[H_s(t), A] \quad (9)$$

is defined as the commutator between any operator A and $H_s(t)$.

Performing the trace over the bath degrees of freedom and then going back to the Schrödinger picture, one obtains from Eq. (7)

$$\dot{\rho}_s(t) = \mathcal{L}_s(t) \rho_s(t) + \mathcal{L}_z[\mathcal{K}(t) + \text{H.c.}], \quad (10)$$

where

$$\mathcal{K}(t) = -i \int_0^t C(t-t') \mathcal{G}_s(t, t') \sigma_z \rho_s(t') dt', \quad (11)$$

H.c. denotes the Hermitian conjugate of its previous term, and $\mathcal{L}_z A = -i[\sigma_z, A]$ for arbitrary operator A , and the bath correlation function at temperature $k_B T = 1/\beta$ is [1, 8]

$$\begin{aligned} C(\tau) &\equiv \text{tr}_b [B(0) B(-\tau) \rho_b] \\ &= \int_0^\infty d\omega J(\omega) \left[\cos(\omega\tau) \coth\left(\frac{\beta\omega}{2}\right) - i \sin(\omega\tau) \right], \end{aligned} \quad (12)$$

with the spectral density $J(\omega) = \sum_k |g_k|^2 \delta(\omega - \omega_k)$.

To deal with Eqs. (10) and (11) without further approximation, one can express the bath correlation function in terms of a sum of exponentials as [10–12]:

$$C(\tau) = \sum_m \alpha_m e^{\gamma_m \tau}, \quad (13)$$

with complex numbers α_m and γ_m that can be obtained from numerical methods.

Substituting Eq. (13) into Eq. (11), one then obtains $\mathcal{K}(t) = \sum_m \mathcal{K}_m(t)$, where $\mathcal{K}_m(t) = -i \int_0^t \alpha_m e^{\gamma_m(t-t')} \mathcal{G}_s(t, t') \sigma_z \rho_s(t') dt'$. By taking the time derivative of $\mathcal{K}_m(t)$ with the help of the property $\frac{\partial}{\partial t} \mathcal{G}_s(t, t') = \mathcal{L}_s(t) \mathcal{G}_s(t, t')$, Eqs. (10) and (11) now become a set of linear equations [12]:

$$\dot{\rho}_s(t) = \mathcal{L}_s(t) \rho_s(t) + \mathcal{L}_z \sum_m [\mathcal{K}_m(t) + \text{H.c.}], \quad (14)$$

$$\dot{\mathcal{K}}_m(t) = [\mathcal{L}_s(t) + \gamma_m] \mathcal{K}_m(t) - i \alpha_m \sigma_z \rho_s(t). \quad (15)$$

We have transformed the time-nonlocal master equation of Eqs. (10) and (11) into the time-local form of coupled Eqs. (14) and (15). These equations are valid even in a strong driving field as the only approximation made in obtaining them is the Born approximation in the weak system-bath coupling limit.

The bosonic bath considered in Refs. [5, 7] is a phonon bath and the spectral density for the piezoelectric phonon coupling considered takes the form

$$J(\omega) = \frac{P}{2} \frac{\omega \omega_c^2}{\omega^2 + \omega_c^2} \left[1 - \text{sinc} \left(\frac{d\omega}{c_s} \right) \right], \quad (16)$$

where P is the piezoelectric electron-phonon coupling strength, ω_c is the bath cutoff frequency, d is the inter-dot separation, and c_s is the transverse speed of sound. The factor $1 - \text{sinc}(d\omega/c_s)$ with $\text{sinc}x = \sin x/x$ describes the oscillations on the frequency scale c_s/d and leads to deviations from the Lorentz-Drude spectral density.

Let us first discuss the behavior of the bath correlation function with $J(\omega)$ given by Eq. (16). The real part of the bath correlation function Eq. (12) coming from the sinc term of Eq. (16) is convergent, while the contribution coming from the Lorentz-Drude term (i.e., the first term) of Eq. (16) [8],

$$\int_0^\infty d\omega \frac{P}{2} \omega \left[\frac{\omega_c^2}{\omega_c^2 + \omega^2} \right] \cos(\omega\tau) \coth \left(\frac{\beta\omega}{2} \right) \quad (17)$$

looks logarithmically divergent at $\tau = 0$ for large frequencies. However, if one does the time integral in Eq. (11) first, one will get additional ω^{-1} power and then the resultant frequency integral will converge [13]. It is then reasonable to assume that the dynamics does not depend appreciably on the very high-frequency bath modes. For our formulation, we would like to evaluate the bath correlation function first and then numerically fit it with multi-exponentials as in Eq. (13). We thus express the Lorentz-Drude spectral density as [14, 15]

$$\frac{P}{2} \frac{\omega \omega_c^2}{\omega^2 + \omega_c^2} \sim \sum_k \frac{4p_k \Omega_k \omega}{(\omega^2 - \Omega_k^2)^2 + 2(\omega^2 + \Omega_k^2) \Gamma_k^2 + \Gamma_k^4} \quad (18)$$

up to a sufficiently high frequency (e.g., up to $100\omega_c$), where the fitting parameters p_k , Ω_k , and Γ_k are real numbers and can be obtained numerically. Then by substituting Eq. (18) into Eq. (16), a high-frequency ω^{-4} power

will converge the integral in Eq. (12). Thus, expressing Eq. (13) as a sum of exponentials becomes achievable. We note that the poles of Eq. (18) correspond roughly to the poles of the response after a sequence of approximations in the Laplace space in Ref. [7]. In the following section, we will introduce a full-polaron method that is free of this divergence problem in its bath correlation functions $C_{ij}(\tau)$. To verify that fitting Eq. (18) up to $100\omega_c$ is reasonable, we compare the case using directly Eq. (16) with that using Eq. (18) in the full-polaron method, and find that both cases give the same dynamical steady-state results presented in this paper.

B. Polaron transformation

To deal with the case of strong system-environment coupling, we first make a polaron transformation to the model Hamiltonian Eq. (1) by [16, 17]

$$H'_T(t) = e^V H_T(t) e^{-V}, \quad (19)$$

where $V = \frac{\Phi}{2} \sigma_z$, and

$$\Phi \equiv 2 \sum_k \frac{g_k}{\omega_k} (b_k^\dagger - b_k). \quad (20)$$

The transformed Hamiltonian can be written as

$$H'_T(t) = H'_s(t) + H'_{sb}(t) + H_b, \quad (21)$$

$$H'_s(t) = -\frac{\epsilon}{2} \sigma_z - \frac{\eta \Delta(t)}{2} \sigma_x - \sum_k \frac{g_k^2}{\omega_k} I, \quad (22)$$

$$H'_{sb}(t) = -\frac{\Delta(t)}{2} (B_x \sigma_x + B_y \sigma_y), \quad (23)$$

where I is an identity matrix, and

$$B_x = (\cosh \Phi - \eta), \quad (24)$$

$$B_y = i \sinh \Phi, \quad (25)$$

are the bath operators in the transformed frame. The parameter η is defined as

$$\begin{aligned} \eta &= \langle \cosh \Phi \rangle_{H_b} \\ &\equiv \text{tr}_b (\rho_b \cosh \Phi) \\ &= \exp \left[-2 \sum_k \left(\frac{g_k}{\omega_k} \right)^2 \coth \left(\frac{\beta\omega_k}{2} \right) \right]. \end{aligned} \quad (26)$$

We have subtracted η , with value $0 \leq \eta \leq 1$, from the bath operator B_x [see Eq. (24)] to make $\langle H'_{sb}(t) \rangle_{H_b} = 0$, and at the same time have added back a corresponding term $-\frac{\eta \Delta(t)}{2} \sigma_x$ to the system Hamiltonian, where $\Delta(t)$ is defined in Eq. (5). This bath-renormalized tunneling term can describe the coherent dynamics of the system at the phonon-dressed energy scale $\frac{\eta \Delta(t)}{2}$. Reference [7] also has a scheme to determine the renormalization of the Rabi frequency via a self-consistent condition that the bath-renormalized system Hamiltonian in the

Laplace space should vanish in the interaction picture. The renormalization of the coherent driving amplitude $\eta\Omega_0$ here is related to the renormalization of the Rabi frequency in Ref. [7]. One can see this by expanding η of Eq. (26) to second order in g_k at zero temperature to obtain $\eta_{2\text{nd}} = 1 - 2 \int_0^\infty d\omega J(\omega) / \omega^2$. Then $\eta_{2\text{nd}}\Omega_0$ is equal to the approximated bath-induced renormalized Rabi frequency Ω_{approx} of Ref. [7]. This relation suggests that their renormalization of the Rabi frequency contains the information of the second-order system-bath coupling contribution while our full-polaron one, i.e., $\frac{\eta\Delta(t)}{2}\sigma_x$, contains not only the second-order but also higher-order contributions.

C. Full-polaron master equation

Even though the original system-bath interaction is strong, the new identified system-bath interaction Hamiltonian $H'_{sb}(t)$ of Eq. (23) that depends on $\Delta(t)$ would be small and could be considered as a perturbation term. Thus, once the parameter η is determined numerically, we then derive perturbatively in the transformed polaron frame a quantum master equation to second order in $H'_{sb}(t)$ from Eq. (21).

The model Hamiltonian, Eq. (1), without the off-diagonal term [i.e., $\Delta(t) = 0$] is a pure-dephasing spin-boson model, and after the polaron transformation, the total Hamiltonian becomes decoupled without the system-environment interaction in the transformed frame. In this case, the reduced system dynamics is described by an exact time-local (time-convolutionless) non-Markovian master equation. So we will adopt for the $\Delta(t) \neq 0$ case a time-local non-Markovian master equation approach [8, 9] to describe the time evolution of the reduced system density matrix,

$$\rho'_s(t) = \text{tr}_b [e^V \rho_T(t) e^{-V}] \quad (27)$$

in the polaron frame for our driven model. Because the initial total density operator is chosen to be $|l\rangle\langle l| \otimes \rho_b$, the polaron transformation displaces the initial bath state to $e^V (|l\rangle\langle l| \otimes \rho_b) e^{-V} = |l\rangle\langle l| \otimes \left(e^{\frac{\Phi}{2}} \rho_b e^{-\frac{\Phi}{2}} \right)$. However, only the steady state is concerned in Refs. [5–7] and the steady-state quantities are independent of the initial states, i.e., does not depend on whether the bath state of the transformed initial state is displaced or not [16, 17]. As a result, we choose, for simplicity, the original undisplaced initial state $|l\rangle\langle l| \otimes \rho_b$ as the initial state in the polaron frame. The full-polaron master equation to second order in $\tilde{H}'_{sb}(t)$ in the interaction picture with respect to $H'_0(t) = H'_s(t) + H_b$ reads [18]

$$\frac{d}{dt} \rho'_s(t) = - \int_0^t \text{tr}_b \left[\tilde{H}'_{sb}(t), \left[\tilde{H}'_{sb}(t'), \rho'_s(t) \otimes \rho_b \right] \right] dt', \quad (28)$$

where $\tilde{H}'_{sb}(t) = \mathcal{G}'_0(0, t) H'_{sb}(t)$. The propagator super-

operator is defined as

$$\mathcal{G}'_j(t, t') \equiv \mathbb{T}_+ \exp \left[\int_{t'}^t \mathcal{L}'_j(t'') dt'' \right] \quad (29)$$

and the Liouville superoperator

$$\mathcal{L}'_j(t) A \equiv -i [H'_j(t), A] \quad (30)$$

is defined as a commutator between any operator A and $H'_j(t)$ with $j = 0$ for the present case. Later we will introduce $\mathcal{L}'_s(t)$ and its corresponding $\mathcal{G}'_s(t, t')$ as defined in Eqs. (30) and (29) for the system alone with the replacement of Hamiltonian $H'_j(t) \rightarrow H'_s(t)$.

Defining $\sigma_1 = \sigma_x$, $\sigma_2 = \sigma_y$, $B_1 = B_x$, and $B_2 = B_y$, performing the trace over the bath degrees of freedom and then going back to the Schrödinger picture, one can write a concise expression for the second-order time-local master equation from Eq. (28) as

$$\dot{\rho}'_s(t) = \mathcal{L}'_s(t) \rho'_s(t) - \sum_{i,j} \left[\frac{\Delta(t)}{2} \mathcal{L}_i D_{ij}(t) \rho'_s(t) + \text{H.c.} \right], \quad (31)$$

where

$$D_{ij}(t) = i \int_0^t C_{ij}(\tau) \frac{\Delta(t')}{2} \mathcal{G}'_s(t, t') \sigma_j dt', \quad (32)$$

with i, j running from 1 to 2, and $\mathcal{L}_i A = -i[\sigma_i, A]$ for any operator A . The explicit expressions for the bath correlation functions $C_{ij}(\tau) = \langle B_i B_j(-\tau) \rangle_{H_b} = \text{tr}_b [B_i e^{-iH_b\tau} B_j e^{iH_b\tau} \rho_b]$ are [18]

$$C_{11}(\tau) = \eta^2 \{ \cosh[r(\tau)] - 1 \}, \quad (33)$$

$$C_{22}(\tau) = -\eta^2 \sinh[r(\tau)], \quad (34)$$

where

$$r(\tau) = -4 \int_0^\infty d\omega \frac{J(\omega)}{\omega^2} \times \left[\cos(\omega\tau) \coth\left(\frac{\beta\omega}{2}\right) - i \sin(\omega\tau) \right]. \quad (35)$$

The other bath cross correlation functions vanish, i.e., $C_{12}(\tau) = C_{21}(\tau) = 0$. Given Eq. (16), both Eqs. (33) and (34) converge at $\tau \geq 0$ for both $\omega \rightarrow \infty$ (due to ω^{-2}) and $\omega \rightarrow 0$ (due to $[1 - \text{sinc}(d\omega)]/\omega^2$) in the integral of Eq. (35). So there is no divergence problem to express, similar to the weak-system-bath-coupling case, each of the bath correlation functions as a sum of exponentials as:

$$C_{ij}(\tau) = \sum_m \alpha_{ij,m} e^{\gamma_{ij,m}\tau}, \quad (36)$$

with complex numbers $\alpha_{ij,m}$ and $\gamma_{ij,m}$ obtained by numerical methods. This enables us to verify the validity of the expression of Eq. (18), and we find that using Eq. (18)

to replace the Lorentz-Drude term gives the same population dynamics and the same time-averaged steady-state results presented here as those obtained directly using Eq. (16).

Inserting Eq. (36) into Eq. (32), one obtains $D_{ij}(t) = \sum_m D_{ij,m}(t)$, where

$$D_{ij,m}(t) = i \int_0^t \alpha_{ij,m} e^{\gamma_{ij,m}\tau} \frac{\Delta(t')}{2} \mathcal{G}'_s(t, t') \sigma_j dt'. \quad (37)$$

After taking the time derivative of Eq. (37), the resultant equation together with Eq. (31) form a set of differential equations:

$$\begin{aligned} \dot{\rho}'_s(t) = & \mathcal{L}'_s(t) \rho'_s(t) \\ & - \sum_{i,j,m} \left\{ \frac{\Delta(t)}{2} \mathcal{L}_i D_{ij,m}(t) \rho'_s(t) + \text{H.c.} \right\}, \end{aligned} \quad (38)$$

$$\dot{D}_{ij,m}(t) = [\mathcal{L}'_s(t) + \gamma_{ij,m}] D_{ij,m}(t) + i \alpha_{ij,m} \frac{\Delta(t)}{2} \sigma_j. \quad (39)$$

Equation (31) or the set of Eqs. (38) and (39) is the full-polaron master equation that will be used for dealing with time-dependent driving field problems, without making both the rotating-wave approximation and the Markovian approximation.

III. NUMERICAL RESULTS

The key quantities we will calculate and compare are the time-averaged steady-state values of the right dot population $\langle M \rangle_0 = \langle |r\rangle \langle r| \rangle_0 = \langle (1 - \sigma_z)/2 \rangle_0$ [7]. The electron charge state or population of the DQD system can be read out by a rf quantum point contact (rf-QPC) in the experiment [5]. To check whether the interaction strength between the DQD and the phonon bath is in the weak-coupling regime, we use the weak-coupling master equation Eq. (14) to obtain the time evolutions of the population $\text{tr}_T[|r\rangle \langle r| \rho_T(t)] = \text{tr}_s[|r\rangle \langle r| \rho_s(t)]$, and the full-polaron master equation Eq. (38) to obtain

$$\begin{aligned} \text{tr}_T[|r\rangle \langle r| \rho_T(t)] &= \text{tr}_T[|r\rangle \langle r| e^V \rho_T(t) e^{-V}] \\ &= \text{tr}_s[|r\rangle \langle r| \rho'_s(t)]. \end{aligned} \quad (40)$$

We wait until the time evolution of the right dot population has reached the steady state, i.e., a steady sinusoidal oscillation, and then take the time average value in the steady state to obtain $\langle M \rangle_0$. In this paper, we refer to the approach using Eq. (14) to calculate the results as the weak-coupling treatment and the approach using Eq. (38) as the full-polaron method. Using the original parameter set adopted in Fig. 4 of Ref. [5], we found that the results of $\langle M \rangle_0$ obtained by our full-polaron method and the weak-coupling treatment cannot fit well the corresponding experimental data. Moreover, the weak-coupling treatment even gives unphysical negative populations. A more detailed comparison

and description about this can be found in Appendix A. If we decrease the system-bath coupling strength from $P = 0.09$ to a small enough value, e.g., $P = 0.008$, the results of the full-polaron method and the weak-coupling treatment approach each other without any negative populations but still deviate from the experimental data [see Figs. 2(d)–2(f) in Appendix A where a simple estimation of the validity criterion for the weak-coupling treatment is also given]. We discuss furthermore in Appendix B the loss of positivity (negative population) problem in second-order master equations and its indication to the breakdown of the weak-coupling assumption. These results suggest that the original parameter set is not in the weak-coupling regime and may require some adjustment.

We notice that except tunneling rate and temperature obtained independently from the experimental data [5], the other parameters are estimated microscopically in Ref. [5] and may be adjusted slightly to obtain a better fitting to the experimental data. We find that with the other original parameters remaining unchanged, by adjusting the interdot separation slightly from $d/c_s = 20/\omega_0$ to $d/c_s = 14.8/\omega_0 \sim 16/\omega_0$ (with the free parameter Ω_0 adjusted correspondingly to $\Omega_0 = 0.038\omega_0 \sim 0.034\omega_0$), a better fit can be obtained. We show for the case of $d/c_s = 16/\omega_0$ in Figs. 1(a)–1(c) the results of the time-averaged steady-state values of the right dot population $\langle M \rangle_0$ as a function of bias ϵ/ω_0 for driving field strengths $\Omega_0 = 0.034 \times 10^n \omega_0$, where $n = \{0, 0.1, 0.2\}$ corresponds to 28 dB, 30 dB, and 32 dB, respectively, in Ref. [5]. The solid lines in Fig. 1 are the experimental data in Fig. 4 of Ref. [5] and the dotted lines represent the full-polaron results. Our full-polaron method can fit well the steplike shoulders on the blue-detuned side of the asymmetric resonance profile. Similar to the fitting result at 32 dB by the theoretical method [7] presented in Fig. 4 of Ref. [5], the fitting result by the full-polaron method (dotted line) in Fig. 1(c) shows a little higher shoulder than the experimental data (solid line). Taking $c_s = 3000 \text{ ms}^{-1}$ for $d/c_s = 16/\omega_0$, we find $d \sim 240 \text{ nm}$. This value of d is within the possible value of the distance between the localized states of the DQD confined by the surface gates in Ref. [5]. We also estimate the interdot separation from the multi-phonon excitation process instead of the single-phonon excitation process in the weak-coupling case and obtain a value consistent with that obtained from our full-polaron result of $d/c_s = 16/\omega_0$ [19].

Our presented results of the time-averaged steady-state population all have sharp resonance peaks at the value about 0.5. However, as described in Ref. [5], the existence of charge noise, when averaged by the rf-QPC, rounds out or smears out the sharper features of the resonance peaks in the experimental data if the resolution around the resonance peaks is not high enough. Therefore, the focus will be on the overall population behavior rather than on the resonance peak values. The line shapes of the resonance peaks exhibit strong phonon-induced and driving-induced asymmetry. The enhanced population in the blue-detuned side of the peaks, where

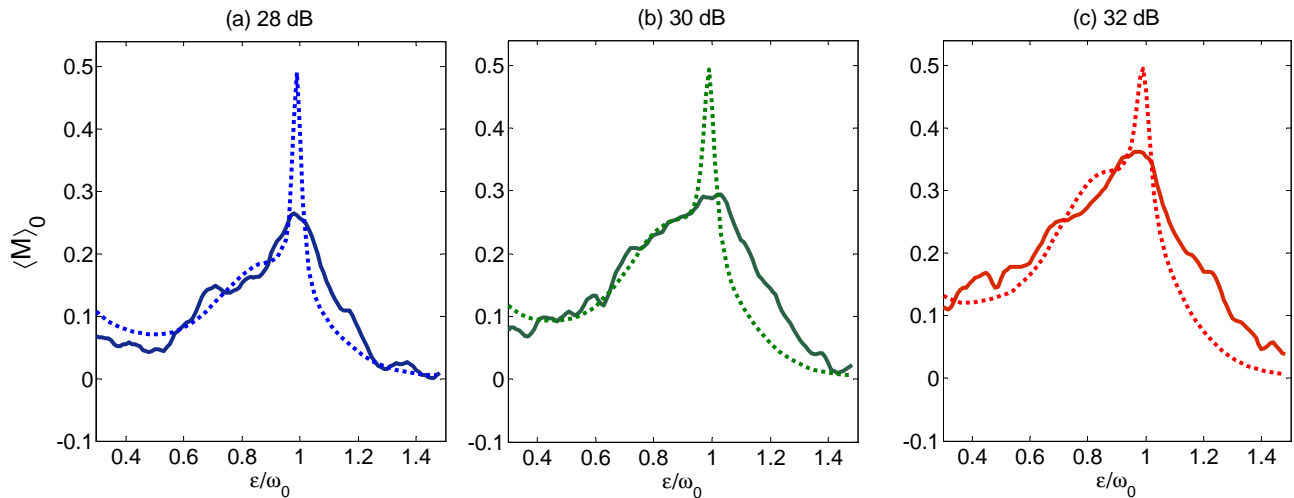


Figure 1. Comparison of time-averaged steady-state population of the right dot $\langle M \rangle_0 = \langle |r\rangle \langle r| \rangle_0$ as a function of bias ϵ/ω_0 normalized by the driving microwave angular frequency $\omega_0 = 2\pi \times 32$ GHz in the driven DQD system for different driving strengths of $\Omega_0 = 0.034 \times 10^n \omega_0$ where $n = \{0, 0.1, 0.2\}$ correspond to (a) 28 dB, (b) 30 dB, and (c) 32 dB, respectively. The experimental data taken from Fig. 4 of Ref. [5] are replotted in solid lines, and the results obtained from the full-polaron master equation method are in dotted lines. The value of interdot separation $d/c_s = 16/\omega_0$, is the fitting value obtained from the full-polaron master equation method. Other parameters used are $P = 0.09$, $\Delta = 0.15\omega_0$, $\omega_c = 2\omega_0$, and $k_B T = 0.12\omega_0$.

the microwave photon energy exceeds the qubit splitting, is the consequence of photon absorption from the driving field accompanied by a Raman phonon emission, leading to a higher rate of excitation than the relaxation rate [6].

IV. DISCUSSIONS

We briefly discuss and compare the theoretical approach used in Refs. [5, 7] with our weak-coupling and full-polaron master equation approaches here. The theoretical method in Refs. [5, 7] involves a Laplace transformation to a second-order time-nonlocal non-Markovian master equation and an energy renormalization scheme with perturbative contributions from the interaction with the bath. So the critical difference between their method and our weak-coupling treatment is their additional renormalization scheme. By comparing their theoretical results in Fig. 4 of Ref. [5] with our weak-coupling results, the obvious effect of their renormalization scheme is the correction of the negative populations when the parameter set ($P = 0.09$) is beyond the weak-coupling regime. References [5, 7] show also that the steplike shoulders come from the spectral density. By expressing $J(\omega)$ as Eq. (18), our weak-coupling treatment can also have the steplike shoulder behaviors on all the results [see Fig. 2 in Appendix A]. In Fig. 1, to fit the steplike shoulders we have decreased the interdot separation slightly from $d/c_s = 20/\omega_0$ to $d/c_s = 16/\omega_0$ for the full-polaron method. We have also checked that the weak-coupling treatment breaks down with negative populations for these parameters because $P = 0.09$ is not small enough.

We discuss next how the perturbative renormalization scheme employed in Refs. [5, 7] can help mitigate the positivity violation problem than the traditional perturbative approach. The positivity violation (negative population values) problem for traditional perturbative second-order master equations is discussed in Appendix B. The perturbative renormalization scheme in Refs. [5, 7] is slightly different from the traditional perturbative approach and is achieved by going to a special basis of the interaction picture via a suitable choice of the dressing Hamiltonian H_D to cancel the bath-induced dispersive shifts (i.e., imaginary parts of the second-order perturbation kernels arising from the bath) so the renormalized system Hamiltonian vanishes in this interaction picture. This determines the dressing system Hamiltonian H_D with two second-order renormalized energies: the diagonal detuning arising from the bath-induced Lamb shift and the off-diagonal Rabi frequency also arising from the bath-induced contribution, which reduces the transition dipole moments. This in turn gives a system energy in the dressed basis closer to the real open system energy than the bare system eigenenergy in the interaction picture of the free Hamiltonian. In summary, in the perturbative scheme (in the system-bath coupling) employed in Refs. [5, 7], the steady-state solutions with second-order corrections to the diagonal elements of the density matrix operator come from two sources. One is from the bath-induced renormalized system Hamiltonian which constitutes the zeroth-order nonperturbative Hamiltonian. This non-perturbative correction is not accessible in the traditional second-order perturbative master equation that works with a bare zeroth-order system Hamiltonian. The other one is from the remaining

second-order perturbation kernels (non-Markovian and non-Lindblad form) that are not canceled in the interaction picture determined by the dressing Hamiltonian. It is the perturbative correction that may induce the second-order positivity violation. But due to the transformation to the basis with respect to the dressing Hamiltonian, the parameter values of their second-order perturbation scheme are altered, resulting in smaller magnitudes of the perturbative kernels or a better perturbation scheme than the traditional weak-coupling perturbation method. Thus smaller fourth-order contributions required for a full second-order solution in the perturbative scheme with renormalized energies employed in Refs. [5, 7] are expected. As a result, it helps mitigate the positivity violation problem or can tolerate a larger parameter regime than the validity regime of the traditional master equation approach. In other words, the renormalization scheme helps lessen the problem of negative right-dot populations for the parameter set in Ref. [5], which is considered beyond the weak-coupling regime. If the system-environment interaction is increased further, this approach will eventually also give negative populations although a less negative value than that by the traditional master equation approach is anticipated.

In contrast, the full-polaron master equation is designed to deal with the strong system-environment coupling case and thus can sustain validity over a much wider parameter regime than the perturbative schemes. The polaron transformation, Eqs. (19) and (20), has a nonperturbative nature in the system-environment coupling. After the polaron transformation, pure-electronic modes are renormalized to polaronic modes with larger effective mass, reducing the coherent tunneling or driving term. The transformed system-bath interaction Hamiltonian that depends on the coherent tunneling or driving term becomes small in the polaron frame and can be treated with regular perturbative master equation approach effectively. Thus the full-polaron master equation can remain valid and go beyond the positivity violation problem for a wider parameter region of the system-environment coupling strength.

Indeed, one can see that there are tiny negative values in the time-averaged steady-state population beside the extra small peaks on the right-hand sides of the dashed lines of the theoretical curves near $(\epsilon/\omega_0) = 1.4$ in Figs. 4(a)–4(c) of Ref. [5], but they are not present in our full-polaron master equation results shown in Fig. 1. This demonstrates that although their renormalization scheme can tolerate a larger parameter regime than our weak-coupling master equation approach [see Figs. 2(a)–2(c) in Appendix A], it still leaves a tiny violation in positivity in that small parameter region. In other words, while the renormalization terms in Refs. [5, 7] contain the contributions from the second-order system-bath coupling, which help lessen the negative population problem, our full-polaron method also contains higher orders as in Eq. (26) and can also capture the effect of multi-bath-quanta processes when the system-bath coupling is not

weak, thus capable of going beyond the positivity violation problem for a wider parameter region.

V. CONCLUSION

We have presented a full-polaron master equation and a weak-coupling master equation to describe the steady-state time-averaged electron population of a driven DQD system interacting with a phonon bath and compare the obtained results with those from a recent experiment and its corresponding theoretical method. We find that the original parameter set used in their experiment and theoretical method is beyond the weak-coupling parameter regime. By using our full-polaron method with a slight change of a single parameter of interdot distance from $d = 20c_s/\omega_0$ to $d = 16c_s/\omega_0$, the experimental results of steplike shoulder behaviors can be fitted rather well. Our full-polaron equation approach does not require the renormalization scheme employed in their weak-coupling theory [7], and can still describe the driving-induced phonon-enhanced phenomena in the experiment. The full-polaron and weak-coupling master equations presented here are efficient tools and can be used to describe, over a quite wide range of parameters in the parameter space, the steady-state behaviors of a driven open quantum system.

ACKNOWLEDGMENTS

H.S.G. acknowledges support from the the Ministry of Science and Technology of Taiwan under Grants No. MOST 106-2112-M-002-013-MY3, No. MOST 108-2627-E-002-001 and No. MOST 108-2622-8-002-016, from the National Taiwan University under Grants No. NTU-CC-108L893202 and No. NTU-CC-109L892002, and from the thematic group program of the National Center for Theoretical Sciences, Taiwan. T.M.S. was supported by the Australian Research Council Centres of Excellence for Engineered Quantum Systems (EQUS, No. CE170100009).

Appendix A: Validity of the parameter set of the driven DQD system used in Ref. [5]

In this Appendix, we discuss how the original parameter set used in the theoretical method [7] to explain the experiment of the driven DQD system in Ref. [5] is not in the weak-coupling regime and may require some adjustment. Figure 2 shows the time-averaged steady-state values of the right dot population $\langle M \rangle_0$ as a function of bias ϵ/ω_0 for driving field strengths $\Omega_0 = 0.034 \times 10^n \omega_0$, where $n = \{0, 0.1, 0.2\}$ corresponds to 28 dB [left panel, (a) and (d)], 30 dB [central panel, (b) and (e)] and 32 dB [right panel, (c) and (f)], respectively, in Ref. [5]. The solid lines (blue, green, and red in the top panel are for

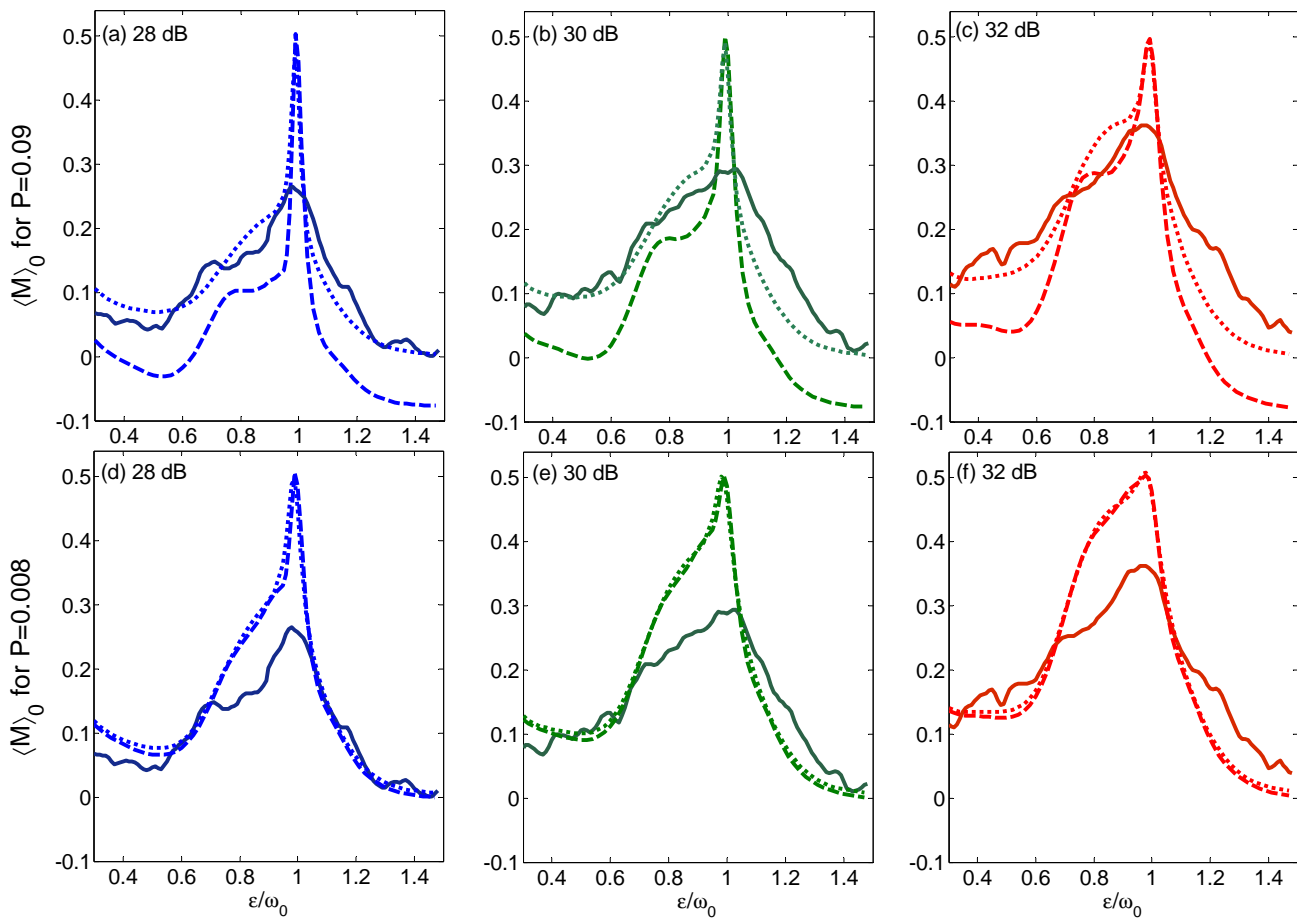


Figure 2. Comparison of time-averaged steady-state population of the right dot $\langle M \rangle_0 = \langle |r\rangle \langle r| \rangle_0$ as a function of bias ϵ/ω_0 normalized by the driving microwave angular frequency $\omega_0 = 2\pi \times 32$ GHz in the driven DQD system for different driving strengths of $\Omega_0 = 0.034 \times 10^n \omega_0$, where $n = \{0, 0.1, 0.2\}$ correspond to 28 dB [left panel, (a) and (d)], 30 dB [central panel, (b) and (e)] and 32 dB [right panel, (c) and (f)], respectively. The experimental data taken from Fig. 4 of Ref. [5] are replotted in solid lines, and the results obtained from the full-polaron and the weak-coupling master equations are in dotted lines and dashed lines, respectively. The value of interdot separation $d/c_s = 20/\omega_0$ is the original parameter value in Ref. [5]. The original value of $P = 0.09$ given in Ref. [5] is used in (a)–(c). If $P = 0.008$ is an order of magnitude smaller, the results of the full-polaron and the weak-coupling methods as shown in (d)–(f) are in good agreement with each other. Other parameters used are $\Delta = 0.15\omega_0$, $\omega_c = 2\omega_0$, and $k_B T = 0.12\omega_0$.

the convenience of comparison the same as those in the bottom panel and in Fig. 1) in Fig. 2 are the experimental data in Fig. 4 of Ref. [5].

By using the original parameter set adopted in Fig. 4 of Ref. [5] [Ω_0 is a free parameter but the ratio of one value to another on a logarithmic scale in decibel (dB) unit is fixed], Figs. 2(a)–(c) show the results of our full-polaron method (dotted lines), the weak-coupling treatment (dashed lines), and the experimental data (solid lines). One can see that they deviate from each other and the weak-coupling treatment even gives unphysical negative populations. Larger deviations between the results of the weak-coupling treatment and the full-polaron method occur in the off-resonance regimes rather than near the resonance peaks. One might be tempted to think that the weak-coupling treatment is close to the full-polaron method near the resonance peaks. In fact, the detailed

dynamics of the weak-coupling treatment deviates from that of the full-polaron method. In other words, because only the time-averaged steady-state populations are compared there, the weak-coupling treatment gives a close result to that of the full-polaron method. But it does not really mean that the weak-coupling treatment is valid near resonance for this set of parameters. In short, these results suggest that the original parameter set is not for processing in the weak-coupling regime because the weak-coupling treatment breaks down.

Actually, the weak-coupling treatment is expected to be valid when the criterion $\max(\Omega_0, |\delta|) \gg \Gamma$ is satisfied, where the detuning $|\delta| = |W - \omega_0|$ and $W = \sqrt{\epsilon^2 + \Delta^2}$. We have obtained $\Omega_0 \approx 0.034\omega_0$ in Figs. 1 and 2, so in the regime of appreciable off-resonance, we have $|\delta| > \Omega_0$. As a result, the validity criterion of the weak-coupling treatment should require the decay rate

$\Gamma \ll 0.034\omega_0$. The decay rate Γ can be estimated by the expression of the coefficient of the decay term in the master equation as $\Gamma/2 \sim \int_0^{\omega_c^{-1}} C(0) dt'$. In estimating the bath correlation function $|C(0)|$, the sinc $(d\omega/c_s)$ term in the bath spectral density $J(\omega)$ with parameters $d/c_s = 14.8/\omega_0 \sim 20/\omega_0$ has small contributions and can be neglected. So in the low- or zero-temperature limit, we have $C(0) \sim \int_0^{\omega_c} (P\omega/2) d\omega = P\omega_c^2/4$, and this leads to $\Gamma \sim P\omega_0$. To satisfy the validity criterion of the weak-coupling treatment of $\Gamma \ll 0.034\omega_0$, we choose as an example $P = 0.008$, one order of magnitude smaller than $P = 0.09$ in the original parameter set, and show the results in Figs. 2(d)–2(f). One can see that the results of the weak-coupling treatment approach to that of the full-polaron method without any breakdown.

However, since no result in Figs. 2(a)–2(c) can fit well its corresponding experimental data (solid line), we conclude that the original parameter set is not in the weak-coupling regime and may require some adjustment.

Appendix B: Positivity violations in second-order master equations

We briefly discuss the problem of negative population results of the weak-coupling master equation in this Appendix.

A density matrix ρ should be positive semi-definite, i.e., $\langle x|\rho|x\rangle \geq 0$ for all states $|x\rangle$. The solution of the reduced system density matrix $\rho_s(t)$ in the master-equation approach for an open quantum system can be guaranteed to be positive semidefinite at all times if the master equation is exact or is of Lindblad form. It has been shown that perturbative second-order (in system-environment coupling strength) time-local [20–24] or time-nonlocal [8, 20, 22, 25–29] master equations may not guarantee yielding a dynamical map with exact complete positivity. In other words, these second-order master equations may not ensure completely positive evolution and may give

unphysical negative eigenvalues of the density-matrix operator after some time if the parameters are beyond their range of validity.

References [20, 21, 23] have shown that the long-time dynamics of order- $2n$ accuracy of a perturbative density-matrix operator requires an order- $(2n+2)$ master equation. In other words, a perturbative master equation to second order in the system-bath coupling strength yields a full-time solution of the density-matrix operator with accuracy of zeroth order. This can lead to second-order violations of positivity in long-time (steady-state) regimes, especially at low temperatures, as the diagonal elements of the reduced density matrix in the energy basis of the free Hamiltonian are not perturbed to the correct second-order values [20–23]. Reference [24] has shown that the positivity violations in the Redfield master equation with time-dependent coefficients (similar to our weak-coupling master equation) occur only in a parameter regime where the perturbative Redfield master equation becomes significantly invalid, i.e., in a parameter regime of larger system-bath coupling strength or larger bath correlation time. This implies that the loss of positivity should in fact be welcomed as an important feature: It indicates the breakdown of the weak-coupling assumption [24].

To correct the positivity problem, one should require a full second-order solution for the diagonal elements (populations) to keep the density-matrix operator positive semi-definite. This can be achieved consistently to second order from a perturbative process through the help of the fourth-order master equation, or a perturbative expansion of the exact solution to second order, or from a nonperturbative process described by a Lindblad master equation.

On the other hand, the perturbative renormalization scheme employed in Refs. [5, 7] and our full-polaron method can help mitigate the positivity violation problem as compared to the traditional perturbative approach (see Sec. IV in the main text for a brief discussion).

-
- [1] H. J. Carmichael, *Statistical Methods in Quantum Optics 1* (Springer, Berlin, 1999).
 - [2] D. P. S. McCutcheon, N. S. Dattani, E. M. Gauger, B. W. Lovett, and A. Nazir, *Phys. Rev. B* **84**, 081305(R) (2011).
 - [3] J. R. Petta, A. C. Johnson, C. M. Marcus, M. P. Hanson, and A. C. Gossard, *Phys. Rev. Lett.* **93**, 186802 (2004).
 - [4] R. Hanson, L. P. Kouwenhoven, J. R. Petta, S. Tarucha, and L. M. K. Vandersypen, *Rev. Mod. Phys.* **79**, 1217 (2007).
 - [5] J. Colless, X. Croot, T. Stace, A. Doherty, S. Barrett, H. Lu, A. Gossard, and D. Reilly, *Nat. Commun.* **5**, 3716 (2014).
 - [6] T. M. Stace, A. C. Doherty, and S. D. Barrett, *Phys. Rev. Lett.* **95**, 106801 (2005).
 - [7] T. M. Stace, A. C. Doherty, and D. J. Reilly, *Phys. Rev. Lett.* **111**, 180602 (2013).
 - [8] H.-P. Breuer and F. Petruccione, *The Theory of Open Quantum Systems* (Oxford University Press, Oxford, 2002).
 - [9] R. Xu and Y. Yan, *J. Chem. Phys.* **116**, 9196 (2002).
 - [10] B. Hwang and H.-S. Goan, *Phys. Rev. A* **85**, 032321 (2012).
 - [11] J.-S. Tai, K.-T. Lin, and H.-S. Goan, *Phys. Rev. A* **89**, 062310 (2014).
 - [12] C.-C. Chen and H.-S. Goan, *Phys. Rev. A* **93**, 032113 (2016).
 - [13] I. Sinayskiy, E. Ferraro, A. Napoli, A. Messina, and F. Petruccione, *J. Phys. A: Math. Theor.* **42**, 485301 (2009).
 - [14] G. Ritschel, J. Roden, W. T. Strunz, and A. Eisfeld, *New J. Phys.* **13**, 113034 (2011).
 - [15] G. Ritschel and A. Eisfeld, *J. Chem. Phys.* **141**, 094101 (2014).

- [16] H.-T. Chang, P.-P. Zhang, and Y.-C. Cheng, *J. Chem. Phys.* **139**, 224112 (2013).
- [17] D. P. S. McCutcheon and A. Nazir, *J. Chem. Phys.* **135**, 114501 (2011).
- [18] D. P. S. McCutcheon and A. Nazir, *New J. Phys.* **12**, 113042 (2010).
- [19] Reference [5] estimated that the first step in right-dot population in the blue-detuned region occurs at $\epsilon \sim 0.75\omega_0$, and estimated $d \sim 280$ nm from the first plateau (local maximum) of $J(\omega)$ at $d\omega/c_s \sim 3\pi/2$, where c_s is the transverse speed of sound, i.e., from the commensuration of the Raman phonon wavelength of an emitted phonon with the interdot distance. So they considered that the enhanced electron-phonon coupling is caused by the single-phonon process. From our full-polaron results, we expect that besides the single-phonon process, the multi-phonon excitation will contribute to the enhanced phonon coupling. While $J(\omega)$ in Eq. (12) in the weak-coupling case exhibits the first plateau at $d\omega/c_s \sim 3\pi/2$ as a local maximum, we note that the critical difference of our full-polaron method from their theory is the effective spectral density $J(\omega)/\omega^2$ in Eq. (35) involved in the bath correlation functions in the transformed frame. The effective spectral density exhibits a global maximum at $d|\delta'|/c_s \sim 3.1$, and when the energy of detuning $\delta' = \sqrt{\epsilon^2 + (\eta\Delta)^2} - \omega_0$ matches this maximum, the phonon coupling is enhanced. This results in the driving-induced phonon-enhanced step-like population features. We note that the first step in right-dot population of our full-polaron fitting results occurs at $\epsilon \sim 0.8\omega_0$. Then taking $c_s = 3000 \text{ ms}^{-1}$, we find the interdot distance $d \sim 3.1c_s/|\delta'| \sim 240$ nm, which is within the possible values allowed by the geometry of the surface gates that define the DQD in the experiment and also gives the value of d/c_s , close to the value of the fitting parameter $d/c_s = 16/\omega_0$ we used for our results.
- [20] C. H. Fleming and N. I. Cummings, *Phys. Rev. E* **83**, 031117 (2011).
- [21] C. H. Fleming, N. I. Cummings, C. Anastopoulos, and B. L. Hu, *J. Phys. A: Math. Theor.* **45**, 065301 (2012).
- [22] C. Fleming and B. Hu, *Ann. Phys.* **327**, 1238 (2012).
- [23] J. Thingna, J.-S. Wang, and P. Hänggi, *J. Chem. Phys.* **136**, 194110 (2012).
- [24] R. Hartmann and W. T. Strunz, *Phys. Rev. A* **101**, 012103 (2020).
- [25] S. M. Barnett and S. Stenholm, *Phys. Rev. A* **64**, 033808 (2001).
- [26] A. A. Budini, *Phys. Rev. A* **69**, 042107 (2004).
- [27] S. Maniscalco, *Phys. Rev. A* **72**, 024103 (2005).
- [28] H.-P. Breuer and B. Vacchini, *Phys. Rev. E* **79**, 041147 (2009).
- [29] B. Vacchini and H.-P. Breuer, *Phys. Rev. A* **81**, 042103 (2010).